

OilseedcropNet: Discriminating Edible Oilseed Crops Using PlanetScope Temporal Dataset

SaloniAwaghade^a, Anil Kumar^{*a}, UttaraSingh^b, Sunil Tiwari^c

^aIndian Institute of Remote Sensing, Dehradun, India

^bCMP Degree College, University of Allahabad

^cBhagwant University, Ajmer

*Corresponding author: A. Kumar <anil@iirs.gov.in>

Received: September 9, 202; Accepted: March 1, 2023; Published: March 26, 2023

Abstract

Objective of this research work was to evaluate the significance of spectral bands at different stages of crop growth while mapping oilseed crops. Study area considered was in the surroundings of Merta, Nagaur, Rajasthan, India. The target oilseed crops for the study were Mustard and Taramira. To handle spectral overlap between these crops, temporal MASVI2 index from PlanetScope data were generated. Optimum number of temporal dates was selected from separability analysis using a temporal indices database. Optimum temporal indices data was classified with OilseedcropNet to map Oilseed crops. Mustard crop found in the field was homogeneous and was mapped as homogeneous fields. Taramira crop fields were not homogeneous, as it has soil patches in between crop patches within the same field. Due to this issue OilseedcropNet, has not mapped Taramira crop fields with acceptable accuracy. Further fuzzy Modified Possibilistic c-Means employing 'Individual Sample as Mean' Training approach was used to map Taramira crop, where each sample served as an input parameter for the model's training. It was observed that OilseedcropNet gave good classification results for homogeneous mustard crop fields with sufficient training data size, but failed to map heterogeneous Taramira crop with small training samples. On the other hand, the MPCM approach using the 'Individual Sample as Mean' training approach gave good classification results for the Taramira crop with fewer training samples. Red and NIR band combination for temporal indices database for mustard crop was found best. For Taramira mapping, Red and NIR bands for the initial stage, while yellow and red bands for later stages were found most effective.

Keywords: MSAVI2, MPCM, 'Individual Sample as Mean', MMD, OilseedcropNet

1. Introduction

Remote sensing has evolved as a multidisciplinary branch of science dedicated to developing a variety of

applications in each and every field. Agriculture is one of the most important industries in the country's economy. Since the start of the civilian remote sensing programme in the United States in the early 1960s, the main areas of interest have been agricultural crop identification and area estimation. In last two decades, remote sensing and GIS technology have been applied to explore agricultural applications like crop classification, soil moisture estimation, crop production forecasting, yield estimation and many more (Congalton, 2015) to overcome the advantages of traditional agricultural techniques and surveys (Mazzia et al., 2020).

Mustard (*Brassica nigra*) is a cruciferous broadleaf annual oilseed crop. It is a rabi season crop that grows quickly with crops ripening in 90 to 100 days. Mustard plants have eight major growth stages during their life cycle: germination, leaf development, stem elongation, inflorescence emergence, flowering, fruit development, ripening, and senescence.

Taramira is grown mostly in Sweden, Germany, France, Canada, and China, but it is said to have originated in South Europe and North Africa. Uttar Pradesh, Rajasthan, Haryana, Punjab, and Madhya Pradesh are the largest rising states in India. Rajasthan has the highest Taramira production in the country. It is primarily grown in marginal and sub-marginal areas with low fertility. Taramira crops thrive in sandy and loamy sand soils. It is cultivated as rainfed crops because of its drought

tolerance capacity (Yadav et al., 2016). The crop's strong root structure allows it to collect rainfall from deep soil layers, making it ideal for areas with minimal or no irrigation. When there is a severe drought or late Rabi rains Taramira is the sole alternative for planting with a poor moisture supply. This crop is often harvested between October and February but it can also be produced as late as the first week of December and still produce significant yields and economic benefits (Yadav et al., 2016).

Crop classification and discrimination is based on the fact that every crop has unique reflectance in different parts of electromagnetic spectrum (Sun et al., 2019). Temporal remote sensing data use different indices such as NDVI (Normalised Vegetation Index), MSAVI (Modified Soil Adjusted Vegetation Index) and LAI (Leaf Area Index) depending on the spectral information of different bands of different sensors and used for mapping specific plants or crops (Mazzia et al., 2020).

This study includes an MSAVI2 index specifically designed to provide more accurate results by reducing soil effects. The use of moderate to advanced spatio-temporal data has made the crop mapping process more efficient and effective (Sun et al., 2019). The rapid growth of learning machines has solved many complex problems and evolved it as a research area of interest. The traditional machine learning techniques require feature extraction as a prerequisite (Lecun et al.,

1998). Deep learning solves the problem of selecting the best feature for a given problem. It solves the problem by automatically extracting features from raw input. Various deep learning models have been actively investigated in the field of agriculture.

Deep learning is a very significant subset of machine learning due to its high performance across various domains (Sabir & kumar, 2022a). Deep learning models have multiple processing layers that learn from data at various levels of abstraction. (Lecun et al., 2015). Convolutional neural networks are an excellent approach to employ deep learning to classify images and have the capability to extract the different features from images. The performance accuracy mostly depends on computational loads and tuning of hyper parameters. Some of the key reasons for considering OilseedcropNet over traditional models are as follows: To begin, the main reason for using OilseedcropNet is the concept of weight sharing, which significantly reduces the number of parameters that must be trained, resulting in improved

2. Vegetation index

Spectral signatures of particular plants are identified using the relationship between reflected, absorbed, and transmitted energy. Spectral signatures are unique to plant species (Gilabert et al., 2002). Vegetation index is the mathematical expression of different spectral band combinations. It is the

generalisation. OilseedcropNet can be trained smoothly and without overfitting because there are fewer parameters. Second, the classification stage was combined with the feature extraction stage, and both stages used the learning process. Third, creating large networks with general artificial neural network models is extremely difficult (ANN) (Indolia et al., 2018). The deep learning models automate the process of classification which in turn reduces both time and manual effort (Sun et al., 2019,).

The study focuses on mapping of edible oil seeds like Taramira and Mustard using temporal dataset of PlanetScope satellites with proposed 1D-CNN based OilseedcropNet. Taramira and Mustard oilseeds crop have been considered because mustard crop fields are homogeneous fields while Taramira crop fields are heterogeneous crop fields for the study area. Overall research objectives were to test how 1D-CNN based OilseedcropNet model works for homogeneous as well as heterogeneous crop fields with small training data samples.

comparison of reflected values at different wavelengths. The primary goals of vegetation indices are to enhance vegetation, remove topographic impacts, and minimise data dimensionality. As a result, vegetation indices use spectral responses in the red to near infrared part of the electromagnetic spectrum to accurately indicate vegetation (Congalton,

2015). Absorption in the red and reflectance in the near infrared spectral bands are indicators of the crop's vigour. It has been observed that the ratio of near infrared to red radiance is a good indicator of the vigour of the crop. Some of these traits are used to distinguish crops. Band rationing also reduces the impression of shadows in the image. Crop classification in agriculture is often done using vegetation indices obtained using red and near infrared reflectance. NDVI (Normalised Difference Vegetation Index) fluctuates with soil color, soil moisture etc. while SAVI (Soil Adjusted Vegetation Index) accounts for differential red and near-infrared attenuation via the vegetation canopy. MSAVI2 helps to reduce the soil effect and maximises vegetation effect (Sabir & Kumar, 2022). The formula of MSAVI2 is given by eq (1).

$$MSAVI2 = \frac{2 * NIR + 1 - \sqrt{(2 * NIR + 1)^2 - 8 * (NIR - RED)}}{2} \dots(1)$$

3. Classification Algorithm of CNN

Convolutional Neural Networks (CNN), commonly referred as ConvNets, were introduced in the 1980s by utilising the ideas of a Japanese scientist named Fukushima, 1988 (Lecun et al., 1998). It is a deep learning algorithm which takes input images, assigns importance (weights and biases) to features present in the image and gives classified output. When the

amount of training data is less or an application is developed with a clear objective, 1D-CNN has shown to perform better (Sun et al., 2019).

Previous studies have shown wide range of applications and popularity of CNN attributes with following advantages and thus preferred (Kiranyaz et al., 2021):

Under equivalent conditions (having same configurations, hyper parameters) computational complexity of 1D-CNN is significantly lower than 2D CNN.

e.g. Suppose an image with size NxN dimension convolve with kernel of size MxM, then it will have computational complexity of $O(N^2 M^2)$ but in corresponding 1D convolution it is $\sim O(NM)$

Networks with shallow architectures are obviously much easier to train and implement because in general, most 1D CNN applications have utilised compact (with 1-2 hidden CNN layers) configurations with networks containing <10K parameters, but practically all 2D CNN applications have employed "deep" architectures with more than 1 M (typically exceeding 10 M) parameters.

Deep 2D CNN training typically necessitates the use of specialised hardware (e.g., Cloud computing or GPU farms). On the other hand, any CPU implementation on a typical computer is practical and rather quick for training small 1D CNNs with few hidden layers (e.g., 2 or less) and neurons (e.g., <50).

Compact 1D CNNs are well-

suitable for real-time and low-cost applications, because of their minimal processing requirements (Kiranyaz et al., 2021).

CNN is an example of a multilayer perceptron (MLP), a feed-forward deep network with multiple layers of neurons. Following 1D-CNN model concept OilseedcropNet model has been proposed and tested in this research work. 1D-CNN based OilseedcropNet performs quite well, when processing data using a grid-like design (Sabir & Kumar, 2022a). It is therefore a well-liked solution for classifying images. In 1D-CNN based OilseedcropNet, there are three main kinds of layers: input layers, hidden layers, and output layers. 1D-CNN based OilseedcropNet employs convolution operation in at least one of the layers to highlight the target class or identify the desired attribute (Sabir & Kumar, 2022a). The input layer, output layer, convolution layer, number of hidden layers, dense layer, flatten layer, Maxpooling, and dropout layer are all components of 1D-CNN based OilseedcropNet basic layer. In order to maintain data format, the input layer acts as an interface between input data and the convolution layer.

3.1 Convolution layer

Convolution layer is the first layer of 1D-CNN based OilseedcropNet. It is a layer of a deep neural network where an input matrix is passed through a convolution filter. A kernel provides the input image, and the weights are

subsequently adjusted to optimize using the training data set. The convolution layer uses a kernel that slides over the input to carry out convolution operations. When the convolutional filter is applied, it is simply replicated across cells such that each is multiplied by the filter (Indolia et al., 2018). Convolution retains the spatial relationship between pixels by learning picture properties from pixel patterns and arrangement. The convolution operations are controlled by the kernel size and activation function. Compressing $n \times n$ non-overlapping groups of neurons from the image results in the information collected from the image being compressed into a single neuron (Sivaraj et al., 2022).

3.2 Activation function

It is used to calculate weighted sum of inputs and biases, which is in turn used to decide whether a neuron can be activated or not. The purpose of the activation function is to introduce non-linearity into the output of a neuron. It is important because if the layers are not stacked on top of each other, the number of layers won't make much of a difference. Activation functions are used to facilitate more complex activities by eliminating the image's concealed information. Depending on the application, a variety of activation functions are possible. In this research work Relu was used as it is significantly used in crop classification (Sabir & Kumar, 2022a). It is a nonlinear or piecewise linear function that will

directly output the input if it is positive; otherwise, it will output zero. It removes negative values, resolving the vanishing gradient issue. (Indolia et al., 2018), eq (2).

$$f(x) = (0, x) \dots (2)$$

3.3 Pooling layer

Pooling layer helps to reduce the dimensionality of feature maps. It reduces the number of parameters to learn and the amount of computation performed in the network. Convolution and pooling layers are frequently stacked one on top of the other in 1D-CNN based OilseedcropNet model architecture. Max Pooling is the method that is most frequently used for reducing a neuron's maximum value from a certain window size of 4 (Indolia et al., 2018).

4. Mathematical detail of Fuzzy Model

MPCM (Modified Possibilistic c-means) is a modified version of traditional PCM classifier. The membership value, which ranges from 0 to 1, is used in fuzzy-based soft classification to determine a pixel's membership grade (Mehrotra et al., 2022). Fuzzy approach divides the pixel into membership values corresponding to classes. Fuzzy c-means (FCM) as base version of algorithm (3) stated that summation of membership values should be equal to one. Furthermore, PCM handles the limitations of FCM. It works on the simple principle of degree of belongingness. MPCM was developed to overcome the limitations of FCM and

PCM, which is sensitive to noise (Mehrotra et al., 2022). It uses possibilistic constraint with no optimization of its parameters. Conventional MPCM uses the mean approach as a training parameter. In MPCM the mean of the samples is used to train the algorithm while in ISM each and every sample is treated as the mean to train the algorithm. While handling heterogeneity within the classes ISM works best (Mehrotra et al., 2022; Sivaraj et al., 2022). Each training sample was collected from the field for training purposes. Here, λ_i was introduced for each training sample to reduce the impact of the noise and outlier's parameter, and the PCM's objective function was modified. The MPCM objective function has been mentioned in equation (3).

$$J_{(U,V)} = \sum_{i=1}^N \sum_{j=1}^C (\mu_{ij})^2 \|x_i - v_j\|^2 + \sum_{i=1}^N \eta_i \sum_{j=1}^C (\lambda_i - \mu_{ij})^m \dots (3)$$

λ_i is taken according to the expression mentioned

$$\lambda_i = \sum_{i=1}^C \exp \{-\alpha \|x_j - \beta_i\|^2\}, \quad \lambda_i > 0 \dots (4)$$

where α is a suitably chosen constant, and in Eq. (4),

mean vector of class c is represented by v_j , N represents the number of pixels, x_i represents i^{th} pixel, and η_j is the bandwidth or resolution or scale parameter, which controls the shape and size of the class as given in Eq. (5)

$$\eta_j = \frac{\sum_{i=1}^N (\mu_{ij})^m \|x_i - v_j\|^2}{\sum_{i=1}^N (\mu_{ij})^m} \dots\dots(5)$$

In this research work, v_j has been considered as an individual sample as mean in place of ‘mean’ to handle heterogeneity.

5. Study area and data used

PlanetScope (3m) data were employed for fine resolution while mapping edible oilseed crops. The rural Merta community in the Nagaur district of Rajasthan, India, was chosen as the study region because it contributes to the agriculture-based production of mustard and Taramira. Merta is located at 26° 38' 55" North, 74° 2' 3" East. The research work was carried out during Rabi season for Mustard and Taramira. Both are Rabi crops, hence their 80–90-day crop cycles span the months of November through March for Mustard and October through January for Taramira, respectively. The research work was conducted in the villages of Katyasani, BhuriyaSani, and Nagaur Tehsil. In these settlements, mustard crop output was abundant, but Taramira was discovered in BasniVyas and Hirankhuri. The study made use of a temporal dataset gathered from PlanetScope with a resolution of 3m.

PlanetScope is a satellite constellation consisting of 130 satellites with a 98° orbital inclination and a daily

repeat cycle. The bands used for the study have been mentioned in Table (1). The data consist of a total 8 bands out of which yellow band was 5th band. The dataset was used for temporal indices generation making confirmed that crop phenology is fully covered. The dataset from Nov to March (2021-22) was considered for the mustard crop life cycle, while the dataset from Oct to Feb (2021-22) was considered for Taramira. The temporal data mentioned in the Table-2 and Table-3 were used in the study. Figure-1 denotes a map of study area (Merta, Nagaur, Rajasthan).

6. Methodology

Preprocessing techniques like resampling sub setting and mosaicking was done on a temporal dataset of PlanetScope. It was then followed by generating temporal MSAVI2 indices using different band combinations for early stage, flowering stage and late stage of crop. From the temporal indices database, samples were marked for target and non-target crops for separability analysis and optimum dates were obtained. Training samples collected were used as input data to train the1D-CNN based OilseedcropNet model for classification. Accuracy assessment was conducted using MMD method.

Pre-processing:

Fine resolution dataset of PlanetScope having 3m resolution were atmospherically corrected cloud free data. Eight band data was mosaicked and a

subset of study area was created. These subset images were used for generating MSAVI2 which were then stacked together to create a temporal MSAVI2 index database.

Temporal index database generation:

Temporal index database using MSAVI2 indices model was generated for all three stages of crop. Table (2) and (3) provide details about different band combinations used for generating temporal MSAVI2 indices.

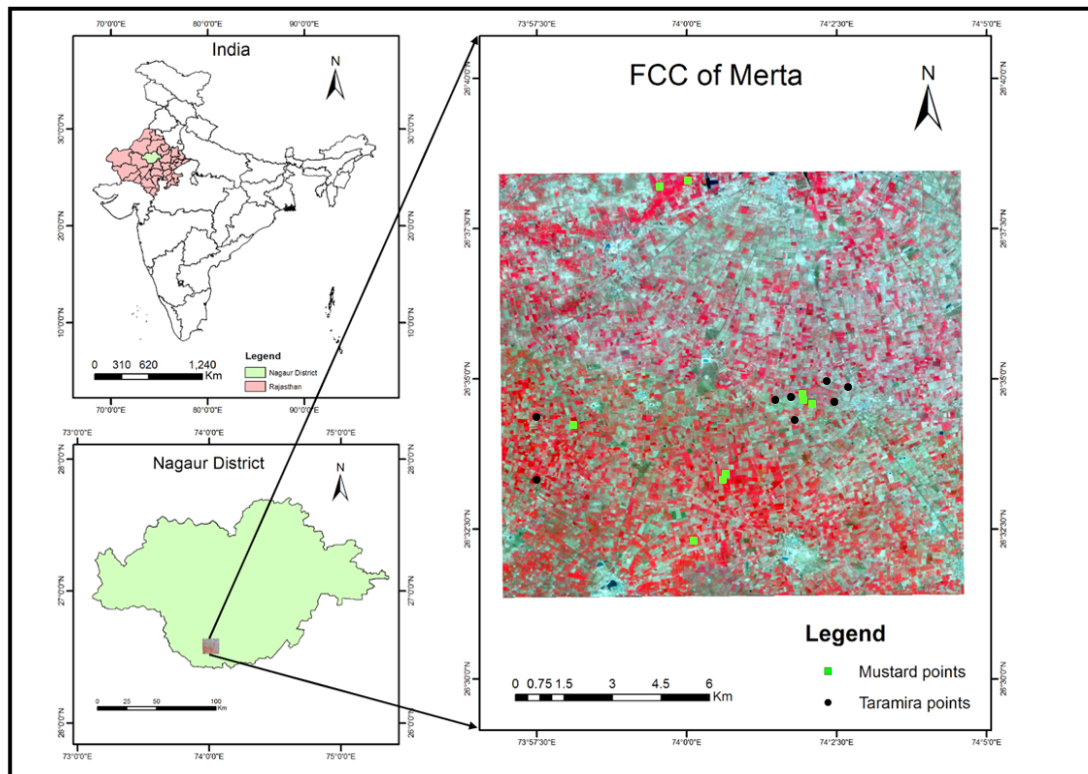


Figure 1: Study area - Merta, Nagaur, Rajasthan

Table 1: PlanetScope Bands used in the study

Bands	Wavelength
Yellow	600 nm – 620 nm
Red	650 nm – 680 nm
RedEdge	697 nm – 713 nm
NIR	845 nm – 885 nm

Case 1 (Red with NIR band)

For the early stage of crop, where chlorophyll content of crop is less and soil is exposed more, reflectance in red is more and peak in NIR. Hence for the early stage, for calculating MSAVI2, the band combination was chosen as Red with NIR, as mentioned in equation (6).

$$MSAVI2_{R/NIR} = \frac{2 * NIR + 1 - \sqrt{(2 * NIR + 1)^2 - 8 * (NIR - RED)}}{2} \dots \dots (6)$$

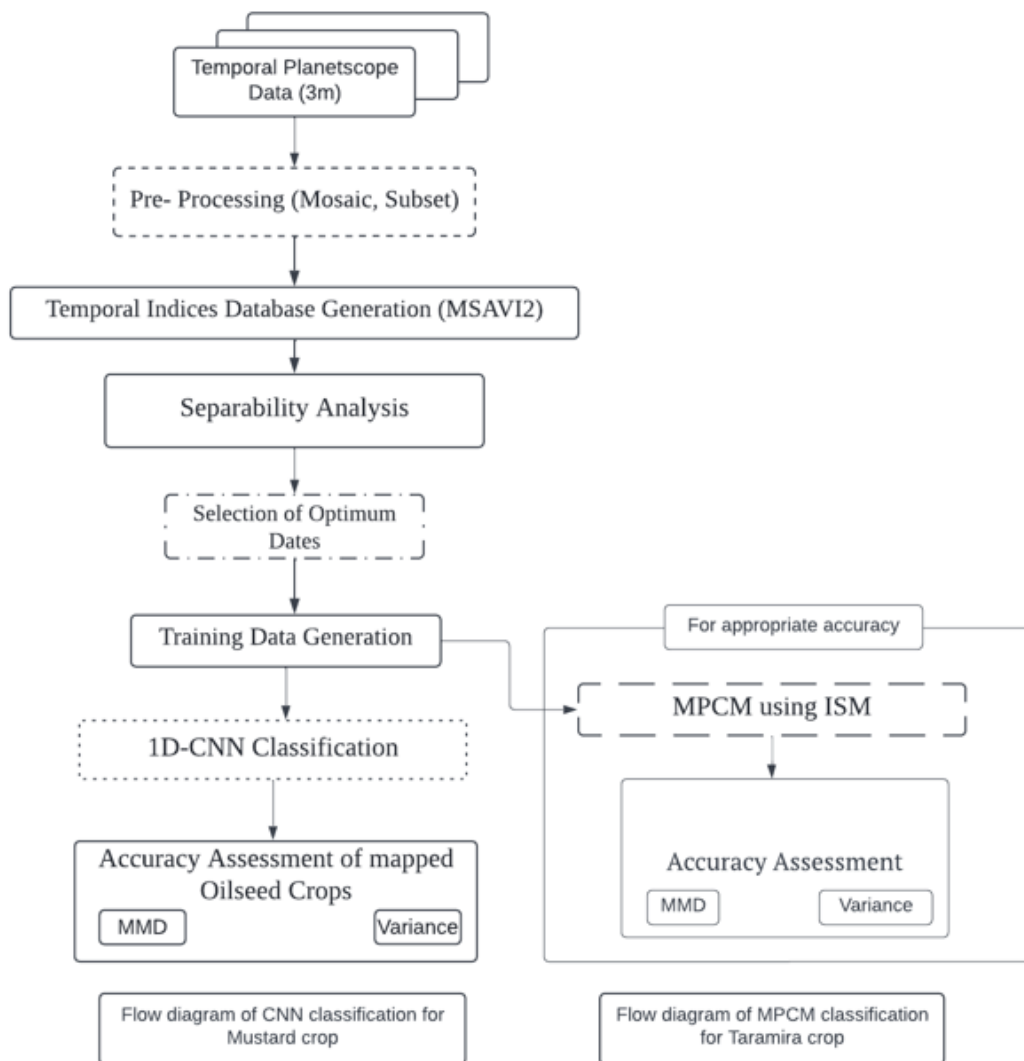


Figure 2: Flow chart of methodology

Case 2 (Red/ Yellow with NIR band)

During the flowering stage, the reflectance in yellow wavelength reaches peak. Modification of the temporal

database for MSAVI2 values was made to highlight the flowering period of the crop. For this red and NIR band combination was replaced with yellow and NIR for

mustard mapping and for Taramira mapping red with yellow was used for the flowering dates. The modified formula is (7) and (8).

$$MSAVI2_{Y/NIR} = \frac{2*NIR+1-\sqrt{(2*NIR+1)^2-8*(NIR-YELLOW)}}{2}$$

....(7)

$$MSAVI2_{Y/R} =$$

$$\frac{2*YELLOW+1-\sqrt{(2*YELLOW+1)^2-8*(YELLOW-RED)}}{2}$$

....(8)

Case 3 (Rededge with NIR band)

The estimated chlorophyll content of plants is determined by the red edge wavelength (Kang et al., 2021). It is mostly used to detect stress in the crop. The red edge moves towards a higher wavelength as chlorophyll concentration rises, and vice versa. Thus, it is utilized in crop mapping to emphasize the crop's planting and harvesting phases (Sabir & Kumar, 2022). For calculating MSAVI2

rededge the modification in MSAVI2 was calculated from equation (9).

$$MSAVI2_{RE/NIR} =$$

$$\frac{2*NIR+1-\sqrt{(2*NIR+1)^2-8*(NIR-REEDGE)}}{2}$$

... (9)

Table 2: Temporal MSAVI2 dataset for Mustard (Nov 2021 - March 2022) with band combinations used

Cases/Dataset	PlanetScope Data
Case 1	Red with NIR band (2 Nov 2021 – 30 March 2022)
Case 2	Red with NIR band (2 Nov 2021 – 21 Nov 2021)
	Yellow with NIR band (18 Dec 2021 – 11 Feb 2022) Red with NIR band (17 Feb 2021 – 30 March 2022)
Case 3	Red with NIR band (2 Nov 2021 – 21 Nov 2021)
	Rededge with band NIR (18 Dec 2021 – 28 Jan 2022)
	Red with band NIR (17 Feb 2021 – 30 March 2022)

Table 3: Temporal MSAVI2 dataset for Taramira (Oct 2021 - Jan 2022) with band combinations used

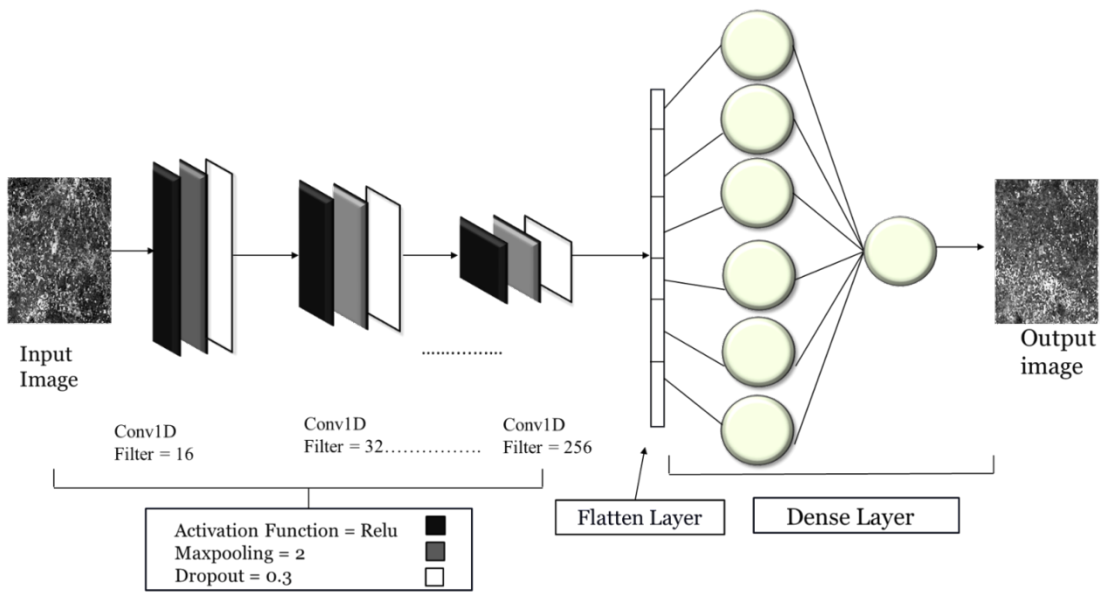
Cases/Dataset	PlanetScope Data
Case 1	Red with NIR band (8 Oct 2021 – 28 Jan 2022)
Case 2	Red with NIR band (8 Oct 2021 – 20 Oct 2021) Yellow with NIR band (11 Dec 2021 – 11 Dec 2022) Red with NIR band (18 Dec 2021 – 28 Jan 2022)
Case 3	Red with NIR band (8 Oct 2021 – 20 Oct 2021) Rededge with NIR band (30 Oct 2021 – 25 Jan 2022) Red with NIR band (28 Jan 2022)

Classification using convolutional neural nets

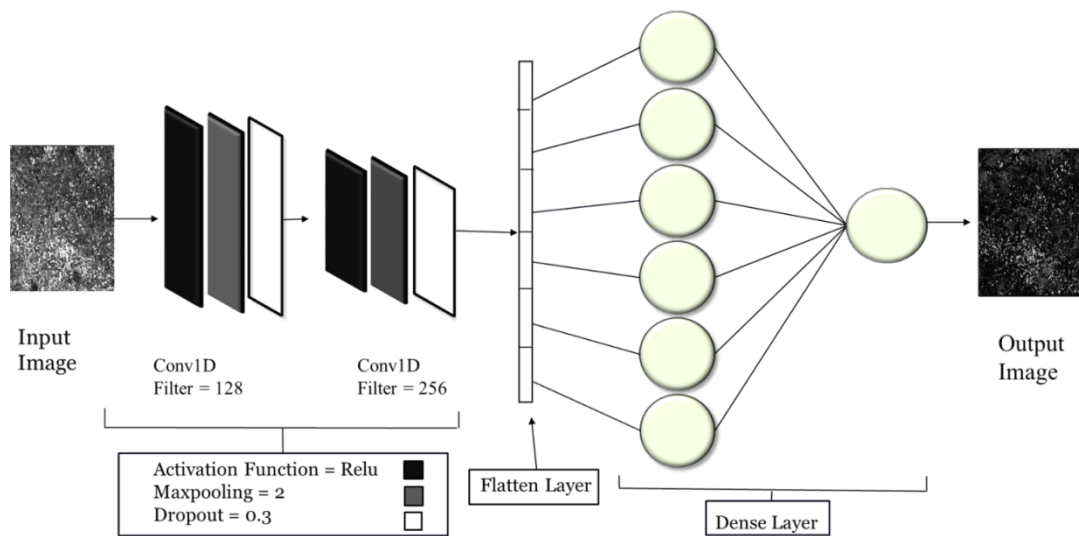
Creation of training data

Training data was created manually based on the 10n rule at pixel locations of oilseed crops. The sample pixels were taken and the homogeneity criteria were followed for selecting the sample pixels from the fields (Sivaraj et al., 2022). Different date combinations were taken into account for both target crops while optimizing temporal data. Therefore training data for both Mustard and

Taramira crops was created separately. The training data was produced using the same pixel positions for the soil modified vegetation index with various combinations of red, yellow, NIR, and red edge bands, and it was stored as a signature file. These signature files were given as input training data for classification through 1D-CNN based OilseedcropNet. Number of samples used for training and testing are mentioned in Table 4.



(a) 1D-CNN based OilseedcropNet architecture for Mustard mapping



(b) 1D-CNN based OilseedcropNet architecture for Taramira mapping

Figure 3: 1D-CNN based OilseedcropNet architectures

Table. 4 Training and Testing samples of both crops used in OilseedcropNet

Samples / Crops	Mustard	Taramira
Training samples	50	40
Testing samples	40	30

Implementation of 1D- based OilseedcropNet

The 1D-CNN based OilseedcropNet model extracts features from sequences of observations and maps the internal features to different activity types(Kang et al., 2021). The training samples i.e., calculated MSAVI2 index values were given as input for classification using CNN. It was then passed through 1D Convolution filter layer keeping varying window size. Each crop has unique physical and biological properties. As a result, multiple models with varying parameters are developed for different crops. For mustard mapping

kernel size starting from 16 x 16 was kept on increasing till 256 x 256 while for Taramira crop kernel size of 128 x 128, 256 x 256 was used sequentially. In both models, the output of the first 1D Convolution layer was given as input for the second 1D Convolution layer and so on. As Relu gives best results for classification, for all layers Relu (Rectified Linear Unit) was a common activation (Kiranyaz et al., 2021). Fig 3(a) shows the architecture of 1D CNN for Mustard mapping and Fig 3 (b) shows architecture of 1D CNN model for Taramira mapping.

Table 5 – MSAVI2 values for mustard considered in the study

Dates	MSAVI2 Values
2-Nov 2021	0.72
21-Nov 2021	0.81
18-Dec 2021	0.86
3-Jan 2022	0.94
13-Jan 2022	0.79
25-Jan 2022	0.83
28-Jan 2022	0.99
1-Feb2022	0.94
4-Feb 2022	0.88
11-Feb 2022	0.92
1-Mar 2022	0.73
10-Mar 2022	0.68
12-Mar 2022	0.66
19-Mar 2022	0.85
22-Mar 2022	0.74
25-Mar 2022	0.84
30-Mar 2022	0.80

Table 6 – MSAVI2 values for Taramira considered in the study

Dates	MSAVI2 Values
8-Oct 2021	0.45
20-Oct 2021	0.54
30-Oct 2021	0.29
11-Nov 2021	0.45
21-Nov 2021	0.47
3-Dec 2021	0.59
11-Dec 2021	0.63
18-Dec 2021	0.54
3-Jan 2022	0.58
13-Jan 2022	0.36
25-Jan 2022	0.54
28-Jan 2022	0.68

7. Results

Table 5 provides the details of temporal image wise MSAVI2 values for Mustard crop while Table 6 includes temporal MSAVI2 values of Taramira crop in the study area. The database of

temporal indices was created by combining the MSAVI2 temporal dates indices that were thus generated. The values highlighted denote the flowering period of that particular crop.

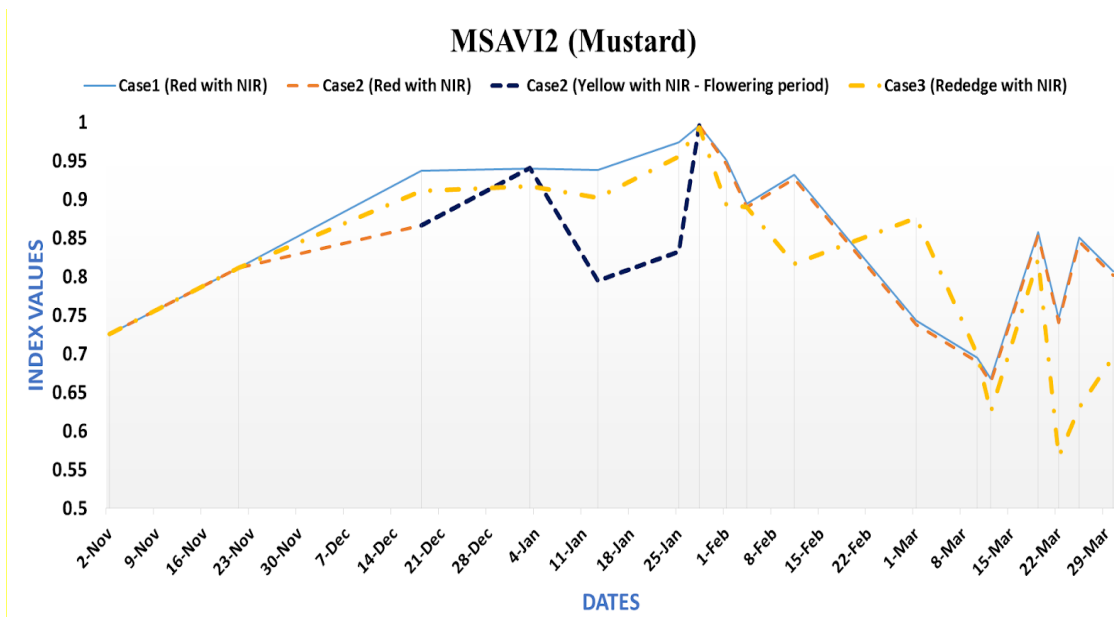


Figure 4: MSAVI2 index curve for Mustard crop

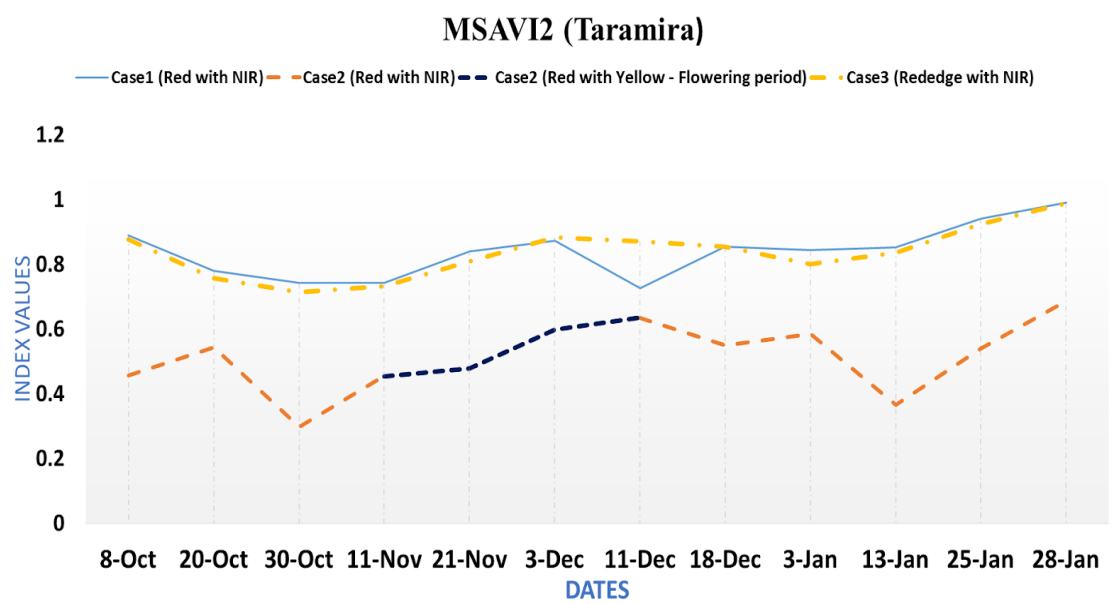


Figure 5: MASVI2 index curve for Taramira crop

For obtaining optimized temporal dates images, in account of the obtained MSAVI2 values, the temporal behaviour of crops across the total 17 dates for Mustard (Table 5) and total 12 dates for Taramira (Table 6) were taken into consideration from their full cycle. Figure

4 displays the indices curves for MSAVI2 values for Mustard crop and Figure 5 denotes graph of Taramira crop. The curves show different phenological stages of both crops.

Separability analysis

To obtain optimum dates, separability analysis was conducted on temporal indices database. Separability analysis was done using Euclidean Distance method. It determines temporal dates that maximized the separation between target crop and non-target crop. Individual layers in the input temporal indices database correspond to dates

indicating particular crop phases of the target crop, which are required for mapping the crop according to its phenology while distinguishing it from other crops. Eight optimum dates were obtained for mustard crop, after performing separability which is highlighted in Table 7 and seven optimum dates were obtained for Taramira mentioned in Table 8.

Table 7- For Mustard minimum eight temporal dates were selected using yellow with NIR band combinations for MSAVI2 variants

No. of Images	Dates	Min separability value
1	10	53
2	9,10	72
3	3, 9,10	86
4	3,8,9,10	97
5	3,5,8,9,10	106
6	3,5,6,8,9,10	113
7	3,4,5,6,8,9,10	115
8	3,4,5,6,8,9,10,11	116
9	3,4,5,6,7,8,9,10,11	117
10	2,3,4,5,6,7,8,9,10,11	117
11	2,3,4,5,6,7,8,9,10,11,12	53
12	1,2,3,4,5,6,7,8,9,10,11,12	72

Table 8- For Taramira minimum seven temporal dates were selected using yellow with red band combinations for MSAVI2 variants

No. of Images	Dates	Min separability value
1	11	54
2	8,11	74
3	8,9,11	89
4	8,9,10,11	97
5	7,8,9,10,11	105
6	3,7,8,9,10,11	106
7	3,6,7,8,9,10,11	107

8	2,3,6,7,8,9,10,11	107
9	2,3,5,6,7,8,9,10,11	108
10	2,3,4,5,6,7,8,9,10,11	108
11	1,2,3,4,5,6,7,8,9,10,11	108
12	1,2,3,4,5,6,7,8,9,10,11,12	108

7.1 Mustard results

All the training samples were collected from the field shown in yellow box is the training field and blue box indicates testing field.

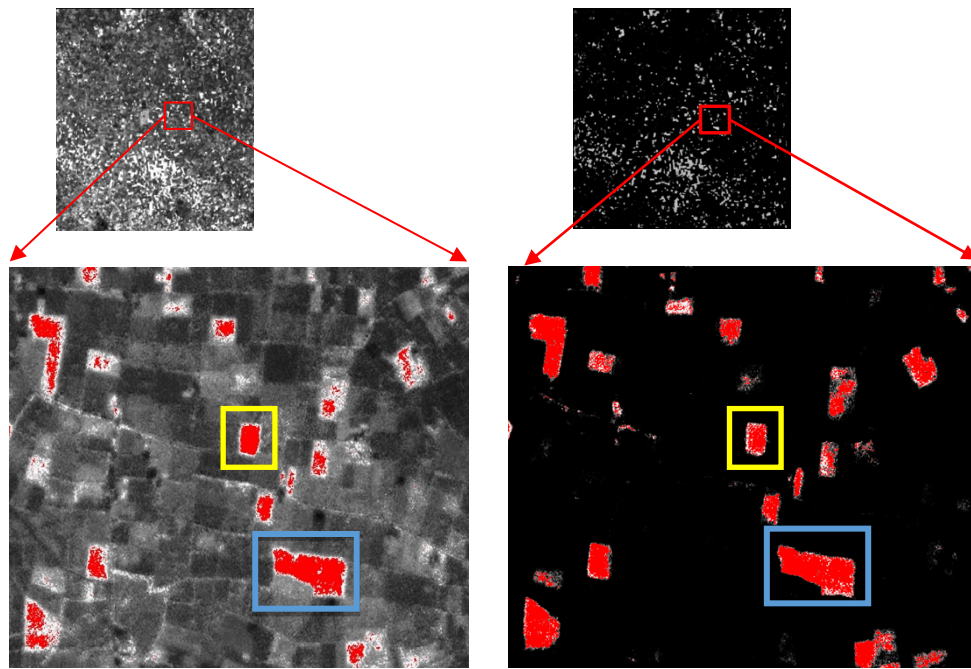
Fig 6, (a) Case 1- Red with NIR shows the result for mustard by 1D-CNN based OilseedcropNet classification for Case 1. By qualitative analysis, the classified output by 1D-CNN based OilseedcropNet gave more homogeneous and uniform fields of mustard covering whole field using Red with NIR band combination for 3m spatial resolution.

In Fig 6, (b) Case 2- Yellow with NIR band indicates the result of 1D-CNN based OilseedcropNet classification for Case 2 considering flowering stage of crop. As compared to (a) Case 1- Red with NIR band output, classification of (b) Case 2- Yellow with NIR band output has been much better by qualitative analysis. 1D-CNN based OilseedcropNet classifies it in an efficient way such that the classified output shows more homogeneous fields and of mustard considering the flowering stage of crop. Hence for Case 2 for mustard mapping, Yellow with NIR band combination is found to be suitable.

Fig. 6 (c) Case 3- Rededge with NIR band indicates the result of Case 3 considering band combination of Rededge with NIR band. These bands combination gives much similar results with Fig 6 (a) Case 1- Red with NIR band where most of the fields are classified clearly by 1D-CNN based OilseedcropNet classification.

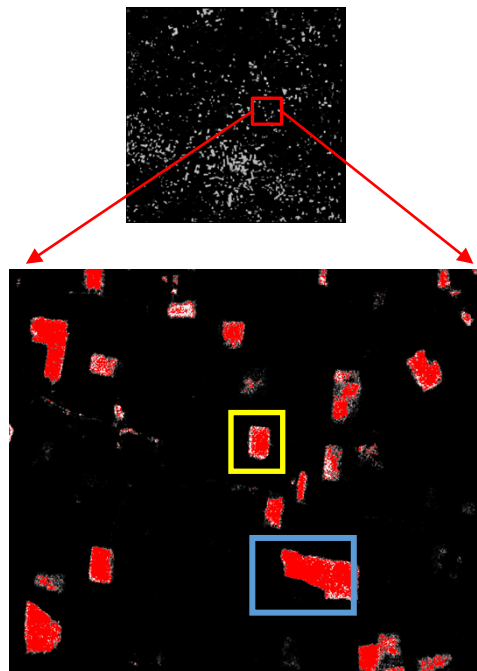
7.2 Taramira results

For all results, the training samples were collected from the field shown in yellow box. The testing field has been indicated with a blue box. Figure7, (a)Case 1- Red with NIR shows the result for Taramira by 1D-CNN based OilseedcropNet classification for Case 1. Fig 7 (b) Case 2-Yellow with NIR indicates the result for Case 2 for Taramira crop at 3m spatial resolution. As there have been a smaller number of pure samples, misclassification was very significant in Case 2. Fig 7 (c) Case 3- Rededge with NIR shows results where band combination of Rededge with NIR was considered. Most of the fields were misclassified by 1D-CNN based OilseedcropNet classification due to increase in heterogeneity.



(a) Case 1- Red with NIR band

(b) Case 2- Yellow with NIR band



(c) Case 3- Rededge with NIR band

Figure 6: Mustard results classified output by 1D-CNN based OilseedcropNet

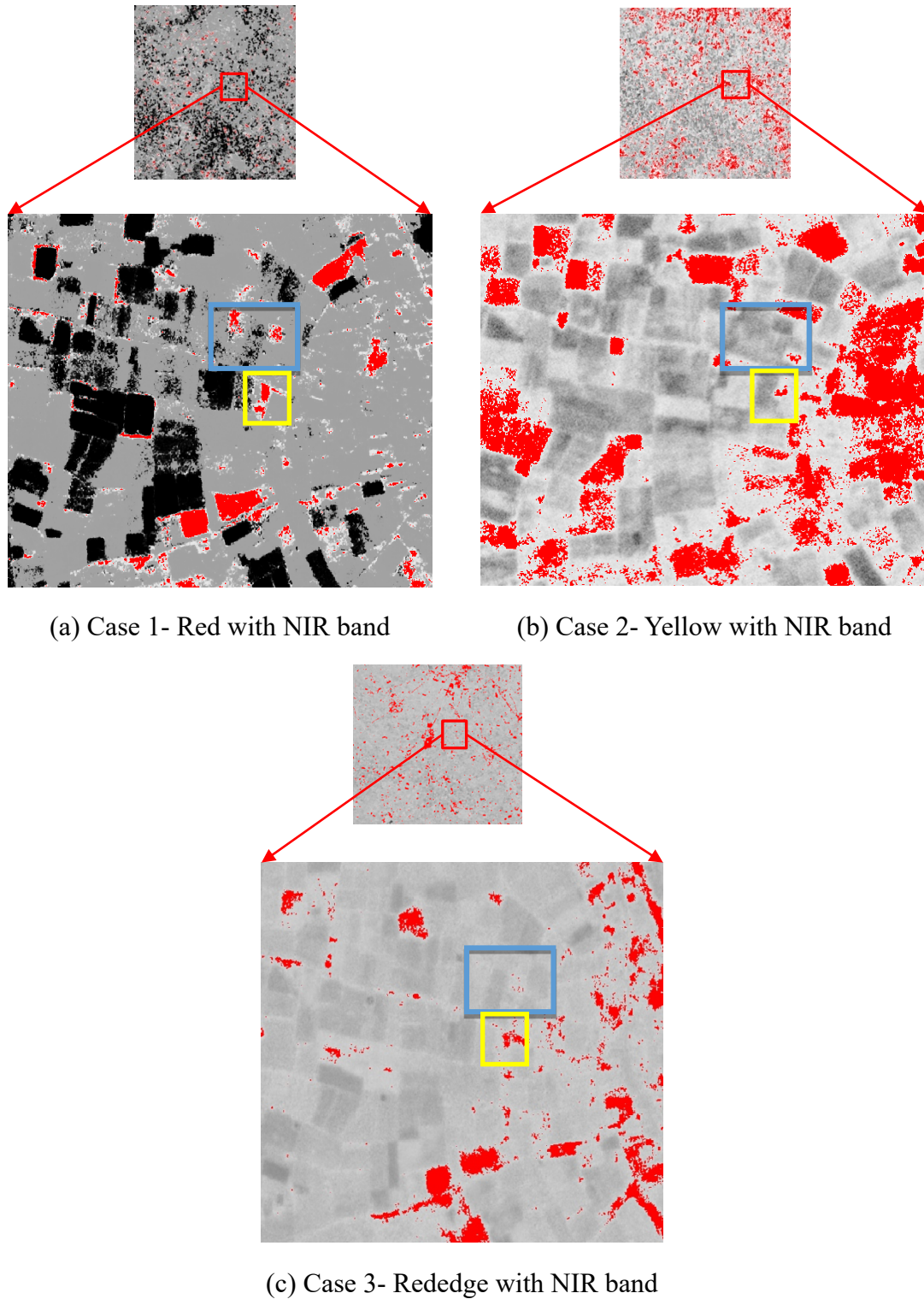


Figure 7: Taramira results classified output by 1D-CNN based OilseedcropNet

8. Discussion

1D-CNN based OilseedcropNet results

The basic architecture of the 1D-CNN based OilseedcropNet model was

created by using convolutional layers, max-pooling layer and dropout layer. The implementation of the 1D-CNN based OilseedcropNet model was done

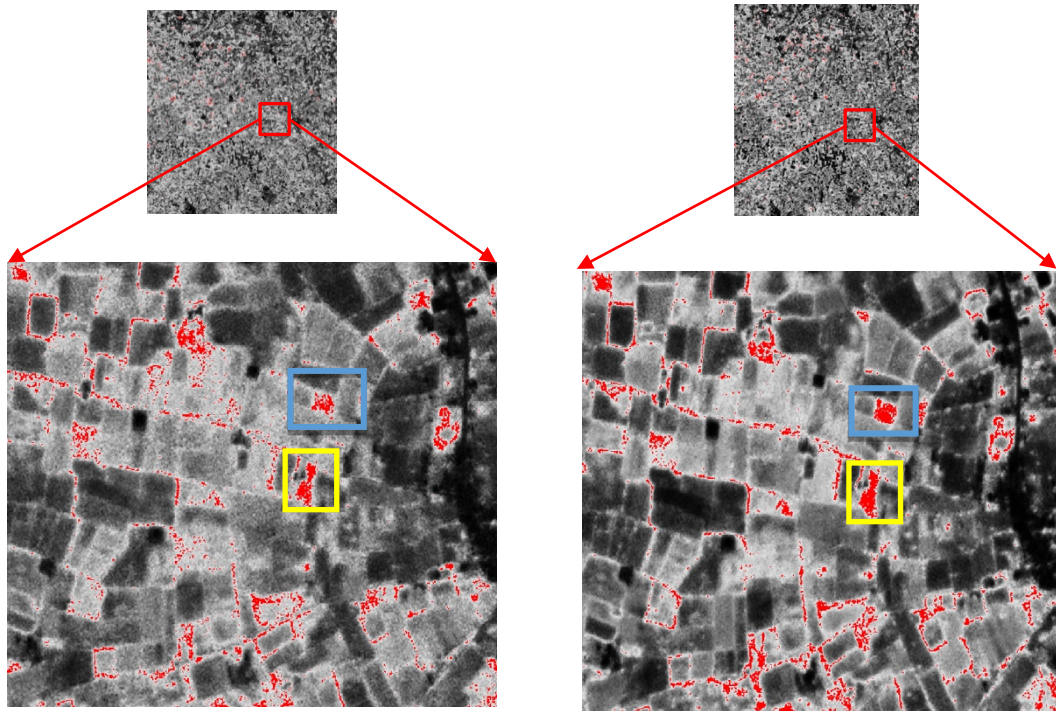
rigorously for hyper parameter tuning so as to get better accuracy. Acceptable hyperparameter adjustments were made to the best-fitting curve, and a comparison analysis was carried out. This procedure was performed continuously until model architecture with optimized hyper-parameters was reached. The accuracy for both oilseed crops was increasing as training samples were increased. Hence the classified results by 1D-CNN based OilseedcropNet were found more homogeneous and accurate. While mapping target crops with increasing training samples, more homogeneous fields were detected. As a result, the output becomes more homogeneous because the mapped fields were identified as a continuous patch, eliminating the possibility of random unclassified pixels within the field's boundary. After a certain point, it was observed in outputs that misclassification was more significant and results started to degrade. This might be due to an excessive number of outliers which causes over classification resulting in noisy output. In the case of mustard due to continuous large fields it was easy to collect a number of samples for training. But for Taramira mapping, as there were less fields it was difficult to collect training samples. Hence heterogeneity was increased causing misclassification of classified output.

Mapping of oilseed crops

Using band combinations in temporal indices as per stage of crop were

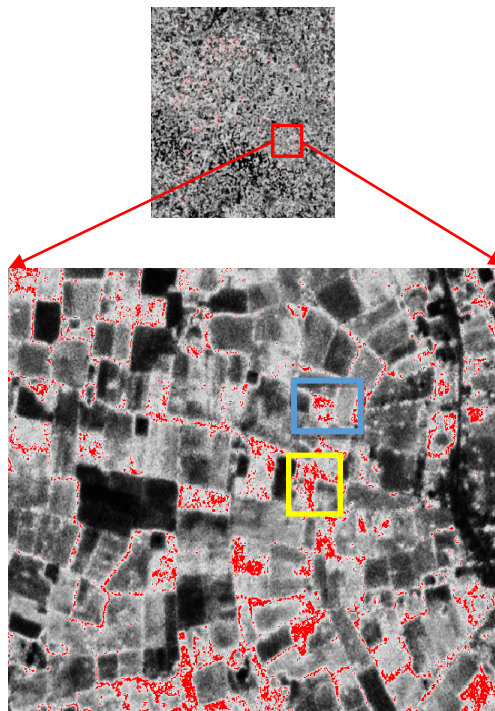
generated for mapping of edible oilseed crops. Because of the green pigments in plant leaves, the spectral reflectance of green vegetation exhibits minimum reflectance in the red wavelength of the electromagnetic spectrum. In the near infrared, reflectance increases considerably. Hence, for mapping of Mustard, Red with NIR band combination was best for fine resolution datasets (Fig 6(a)Case 1- Red with NIR). Taramira is the only alternative for farmers on soils with natural moisture present, and not having irrigation facility as well as late Rabi session rains. Due to non-availability of water to Taramira crop, fields of Taramira crop are non-uniform. Hence collection of pure samples was challenging task within Taramira crop fields and this increases heterogeneity within Taramira crop fields which leads to misclassification. Due to a smaller number of samples possible to collect for training of Taramira crop class, misclassification was observed significantly in all output classified images Fig 7 generated using 1D-CNN based OilseedcropNet. 1D-CNN based OilseedcropNet deep learning model requires little large training samples. To overcome this misclassification problem, another classification approach was used, i.e., fuzzy MPCM, with ISM training approach. Despite of less samples used for classification, MPCM classifier with ISM training approach gave more accurate results (Figure 8). By quantitative analysis the Yellow with Red band combination results Fig 8 (b) were found to

be the best band combination for mapping of Taramira.



(a) Case 1- Red with NIR band

(b) Case 2- Yellow with Red band



(c) Case 3- Rededge with NIR band

Figure 8: Results of MPCM with ISM training approach

Results of MPCM with ISM training approach

In Figure 8, the training samples

were collected from the field shown in yellow box as training field and blue box indicates testing field. Fig8(a) Case 1- Red

with NIR band denotes classified output by MPCM using ISM training approach for Case 1. Comparing the results of Fig 7(a) Case 1- Red with NIR band and Fig 8(a) Case 1- Red with NIR band, the results by ISM were better by qualitative analysis i.e., Fig 8(a). The classified output by MPCM using ISM training approach gave homogeneous and uniform fields of Taramira using Red with NIR band combination for 3m spatial resolution. In Fig 8(b) Case 2 – Yellow with Red band shows the result classification for Case 2 considering the flowering stage of Taramira crop.

Comparing results Fig 7(b) Case 2- Yellow with NIR band and Fig 8(b) Case 2- Yellow with Red band, the results by MPCM using ISM training approach has been better by qualitative analysis i.e., Fig 8(b) Case 2- Yellow with Red band. The classification gives more homogenous field which is not much clearly classified in Figure 7(b). Fig 8(c) Case 3- Rededge with NIR band depicts the classification of MPCM using ISM for Case 3 using a band combination of Rededge and NIR band. Because ISM solves the problem of heterogeneity, this band combination delivers much better results.

Table 9 - Accuracy assessment by MMD

Cases/Crop	Mustard	Taramira
Case 1	0.0027	0.03
Case 2	0.01	0.0078
Case 3	0.012	0.012

Table 10 - Assessment for homogeneous output through variance

Cases/Crop	Mustard	Taramira
Case 1	0.000096	0.00073
Case 2	0.000051	0.00018
Case 3	0.00025	0.0010157

Accuracy assessment

The result was evaluated by the Mean Membership Difference (MMD) approach which gives the difference between training and testing fields. The

accuracy of the classification was determined by the difference between the mean values within a class and between classes. The optimum vegetation index for creating a database of temporal indices

and choosing the right band combination with related weight estimate to identify Mustard and Taramira crops, while optimizing temporal images for early stage, flowering stage and late stage was examined by the MMD approach. Mostly, if the MMD value is lower within the class and higher with non-interested classes then accuracy is considered as high; otherwise, it is low. The table shows MMD accuracy results for mustard and Taramira while Table 10, describes variance for both crops. The values highlighted are the best results for each crop, having least variance values.

9. Conclusion

This research work was conducted to find suitable band combinations to generate temporal indices to be used for edible oilseed crops classification. First, a database of temporal indices was created using the MSAVI2 index, which matches the structure and features of the target crop by decreasing the influence of soil brightness on index values.

Three alternative MSAVI2 index cases were studied encompassing crop phenology of both oilseed crops with varying temporal precision, namely Case 1 with Red and NIR band combination, Case 2 with Yellow and NIR for mustard and Yellow with Red for Taramira, while Case 3 with Rededge and NIR band combination. To better highlight it through separability analysis, temporal datasets for each MSAVI2 variation were constructed

using different phenological periods of the target crop. The ground truth from the field work was used to label training samples on the temporal indices databases and classification was performed using 1D-CNN based OilseedcropNet deep learning model.

Each time, the model was run with a different amount of training samples and the influence on the results was investigated. It was observed that for mapping mustard crop, among MSAVI2 index variants, Red with NIR band combination was found to have best results. After analysing results of 1D-CNN based OilseedcropNet classification for Taramira crop, it was found that misclassification is a significant issue due to training samples. To solve this problem fuzzy MPCM using ISM training approach was applied. The MPCM using ISM training approach takes into account each training sample separately and equally. Hence, for Taramira mapping, Red with NIR band combination for initial stage and later stage Yellow with Red for late stage of crop were found to be the best band combination.

According to the results, the 1D-CNN based OilseedcropNet model outperformed for particular crop classification when training data is more specially for Mustard crop mapping. Deep learning models show significant potential in higher levels of crop classification and might be used for level-4 classification as well. In terms of handling variability within a crop class, the MPCM classifier

using the ISM training approach performed similarly to the deep learning model. A critical selection of dates for the target classes may be performed in the

future to improve the classification results provided by 1D-CNN based OilseedcropNet. Also, classification with 2D CNN can be explored for future studies.

Acknowledgments

Authors are thankful to reviewers as well as editor for providing critical comments, in improving the manuscript.

References

- [1] Congalton, R. G. (2015). Remote Sensing and Image Interpretation. 7th Edition. In Photogrammetric Engineering & Remote Sensing (Vol. 81, Issue 8). <https://doi.org/10.14358/pers.81.8.615>
- [2] Gilabert, M. A., González-Piqueras, J., García-Haro, F. J., & Meliá, J. (2002). A generalized soil-adjusted vegetation index. *Remote Sensing of Environment*, 82(2–3), 303–310. [https://doi.org/10.1016/S0034-4257\(02\)00048-2](https://doi.org/10.1016/S0034-4257(02)00048-2)
- [3] Indolia, S., Goswami, A. K., Mishra, S. P., & Asopa, P. (2018). Conceptual Understanding of Convolutional Neural Network- A Deep Learning Approach. *Procedia Computer Science*, 132, 679–688. <https://doi.org/10.1016/j.procs.2018.05.069>
- [4] Kang, Y., Hu, X., Meng, Q., Zou, Y., Zhang, L., Liu, M., & Zhao, M. (2021). Land cover and crop classification based on red edge indices features of gf-6 wfv time series data. *Remote Sensing*, 13(22), 1–22. <https://doi.org/10.3390/rs13224522>
- [5] Kiranyaz, S., Avci, O., Abdeljaber, O., Ince, T., Gabbouj, M., & Inman, D. J. (2021). 1D convolutional neural networks and applications: A survey. *Mechanical Systems and Signal Processing*, 151, 107398. <https://doi.org/10.1016/j.ymssp.2020.107398>
- [6] Lecun, Y., Bengio, Y., & Hinton, G. (2015). Deep learning. *Nature*, 521(7553), 436–444. <https://doi.org/10.1038/nature14539>
- [7] Lecun, Y., Bottou, L., Bengio, Y., & Ha, P. (1998). LeNet. *Proceedings of the IEEE*, November, 1–46.
- [8] Mazzia, V., Khaliq, A., & Chiaberge, M. (2020). Improvement in land cover and crop classification based on temporal features learning from Sentinel-2 data using recurrent-Convolutional Neural Network (R-CNN). *Applied Sciences (Switzerland)*, 10(1), 1–23. <https://doi.org/10.3390/app10010238>
- [9] Mehrotra, S., Kumar, A., Roy, A., Kushwaha, S. P. S., & Singh, R. P. (2022). Studying dual-sensor time-series remote sensing data for *Dalbergia sissoo* mapping in a Lesser Himalayan area. 16(3), *Journal of*

- Applied Remote Sensing. 1–20.
<https://doi.org/10.1117/1.JRS.16.034521>.
- [10] Sabir, A., & Kumar, A. (2022). Harvesting Information Extraction using Sentinel-2 and CubeSat temporal data for Medicinal Psyllium Husk Crop. 16(1), Journal of Geomatics.45–54.
- [11] Sabir A. and Kumar A., (2022a), Optimized 1D-CNN model for medicinal Psyllium Husk crop mapping with temporal optical satellite data, Ecological Informatics, <https://doi.org/10.1016/j.ecoinf.2022.101772>.
- [12] Sivaraj, P., Kumar, A., & Koti, S. R. (2022). Training concepts in Noise Clustering Classifier -A case study for Pigeon Pea crop mapping. Remote Sensing Applications: Society and Environment, 26(March), 100736.
<https://doi.org/10.1016/j.rsase.2022.100736>
- [13] Sivaraj, P., Kumar, A., Koti, S. R., & Naik, P. (2022). Effects of Training Parameter Concept and Sample Size in Possibilistic c-Means Classifier for Pigeon Pea Specific Crop Mapping. Geomatics, 2(1), 107–124.
<https://doi.org/10.3390/geomatics2010007>
- [14] Sun, J., Di, L., Sun, Z., Shen, Y., & Lai, Z. (2019). County-level soybean yield prediction using deep CNN-LSTM model. Sensors (Switzerland), 19(20), 1–21.
<https://doi.org/10.3390/s19204363>
- [15] Yadav, S., Jakhar, M., & Yadav, L. (2016). Response of taramira (*Eruca sativa*) to varying levels of FYM and vermicompost under rainfed conditions. Journal of Oilseed Brassica, 1(1), 49–52.
- [16] Wu, Xiao-Hong & Zhou, Jian-Jiang. (2006). An Improved Possibilistic c-Means Algorithm Based on Kernel Methods. 783-791.
https://doi.org/10.1007/11815921_86
- [17] Qi J., A. Chehbouni, A. R. Huete, Y.H. Kerr and S. Sorooshian (1994). A modified soil adjusted vegetation index. Remote Sensing of Environment, 48(2), 119–126.
[https://doi.org/10.1016/0034-4257\(94\)90134-1](https://doi.org/10.1016/0034-4257(94)90134-1)
- [18] Huete, A.R. (1988) A Soil Adjusted Vegetation Index (SAVI). Remote Sensing of Environment, 25, 295-309.
[http://dx.doi.org/10.1016/0034-4257\(88\)90106-X](http://dx.doi.org/10.1016/0034-4257(88)90106-X)